DOI: 10.1002/anie.201007121

Controlled Evaporation

One-Step Self-Assembly, Alignment, and Patterning of Organic Semiconductor Nanowires by Controlled Evaporation of Confined Microfluids**

*Zhongliang Wang, Rongrong Bao, Xiujuan Zhang, Xuemei Ou, Chun-Sing Lee, Jack C. Chang, and Xiaohong Zhang**

Organic semiconductors, which have unique electronic and optical properties that differ from those of their inorganic counterparts, have attracted intense attention for potential applications in optoelectronic devices such as organic light-emitting diodes (OLEDs),[1,2] organic field-effect transistors (OFETs),[3–6] organic solar cells (OSCs),[7–9] and gas sensors.[10,11] Numerous reports have indicated that organic semiconductor molecules predominantly aggregate and self-assemble into one-dimensional (1D) nanowires or nanorods along the direction of π–π stacking or other directional intermolecular interactions.[12–16] Owing to excellent performance in carrier transport, such one-dimensional nanostructures may serve as attractive building blocks in future organic electronic applications.[17–21] However, to fabricate practical devices on a large scale, a major challenge is to design a method to deposit and align a large number of such nanowires in a desired position. In most cases, nanostructures self-assembled directly from solution tend to be distributed in a macroscopically random fashion on the substrate. Disordered alignment of organic semiconductors may significantly increase the overall cost due to material consumption and also result in poor performance of electronic devices.[22] Therefore, a facile deposition and patterning method for organic semiconductor molecules is highly desirable. To date, several strategies for alignment of 1D nanowires have been investigated, including the Langmuir–Blodgett technique,[23–26] electric or magnetic field assisted alignment,[27–31] dip coating,[32–34] electrostatic alignment,[35] and so on. However, these methods usually require an external facility and are limited in producing large-area ordered patterns.

In recent years, evaporation-induced self-assembly (EISA) has been reported to prepare well-ordered 2D patterns.[36–39] The EISA method depends on the simple fact that a drop of colloidal solution always leaves a ringlike deposit at the perimeter. During the evaporation process, the loss of solvent mainly occurs at the contact line, and an outward capillary flow carries the solvent and dispersed solute from the interior to the contact line. Therefore, the key parameter to achieve well-ordered 2D patterns is an efficient method to control the contact line. Recently, Lin et al. reported a simple method for controlling droplet evaporation in a confined geometry, which leaves behind well-organized gradient concentric ring patterns.[40–42] With a spherical lens on the substrate, the contact line is well controlled and hence gradient concentric rings are obtained. However, the as-prepared patterns are usually amorphous and no specific nanostructures are formed because of the hard-to-crystallize materials used in evaporation process, such as polymer and inorganic quantum dots (QDs). On the other hand, organic semiconductor molecules can easily self-assemble into 1D nanostructures by evaporation.[43,44] We have developed a facile method to prepare aligned organic nanowires on a solid substrate or liquid/liquid interface based on the EISA method.[33,45] With the aid of solvent evaporation, self-assembly of molecules and alignment of as-obtained nanostructures can be combined to produce a large-area ordered pattern of organic nanowires or films. However, the method wastes a lot of solvent, and the contact line is not easy to control. We have now integrated the EISA method with the concentric ring patterns of Lin et al., so that simultaneous self-assembly, alignment, and patterning of organic semiconductor nanowires can be achieved in one step. Here we demonstrate such a facile approach to fabricate large-scale concentric arrays of nanowires by solvent evaporation in a confined geometry.

N,*N*′-Dimethylquinacridone (DMQA) was selected as a nonvolatile solute in this experiment. It is an industrially important red organic dye with intense fluorescence, which is widely used in photovoltaic and other organic electroluminescent devices.[46–48] It was synthesized according to the reported procedure[49] and was purified twice by vacuum sublimation. Concentric ring patterns of DMQA nanowires were prepared from chloroform solutions of DMQA with concentrations of 0.2, 0.1, and 0.05 mmol L^{-1}. The confined

[*] Z. L. Wang, R. R. Bao, X. M. Ou, Prof. J. C. Chang, Prof. X. H. Zhang
Nano-organic Photoelectronic Laboratory and Key Laboratory of Photochemical Conversion and Optoelectronic Materials
Technical Institute of Physics and Chemistry
Chinese Academy of Sciences, Beijing (China)
E-mail: xhzhang@mail.ipc.ac.cn
X. J. Zhang
Functional Nano & Soft Materials Laboratory (FUNSOM) and Jiangsu Key Laboratory for Carbon-Based Functional Materials & Devices, SooChow University, Suzhou (China)
Prof. C. S. Lee
Center of Super-Diamond and Advanced Film (COSDAF) and Department of Physics and Materials Science
City University of Hong Kong, Hong Kong SAR (China)

[**] This work was supported by the National Basic Research Program of China (973 Program, grant nos.2007CB936000 and 2010CB934500), the National Nature Science Foundation of China (grant nos. 50825304, 91027021 and 50903059).

Supporting information for this article is available on the WWW under http://dx.doi.org/10.1002/anie.201007121.

geometry, constructed in accordance with a previous report,[40] consisted of a glass slide and a spherical lens made of fused silica with a diameter of about 1 cm. The two surfaces were brought into contact and a drop of about 150 μL of DMQA solution was dropped into the gap between slide and lens. A steady upstream of nitrogen gas was blown nearby the setup to help remove the solvent. The whole evaporation process was performed at room temperature inside a fume cupboard, so that the direction and rate of solvent evaporation could be well controlled (Figure 1 a). After the solution was dried on the substrate, it left a number of ordered rings of nanowires which aligned and formed concentric rings on both surfaces, as shown schematically in Figure 1 b.

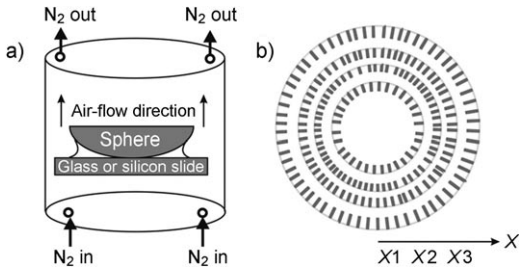

Figure 1. a) Illustration of sphere-on-flat evaporation setup and b) representation of as-prepared concentric rings of organic nanowires.

Figure 2 shows optical micrographs and SEM images of the as-prepared concentric rings prepared at a concentration of 0.10 mmol L^{-1}. Concentric rings of remarkable regularity formed over a large scale of several hundred micrometers.

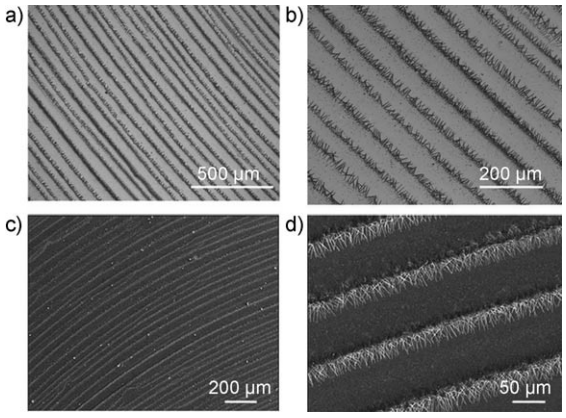

Figure 2. a,b) Optical micrographs and c,d) SEM images of the concentric rings of DMQA nanowires formed during solvent evaporation.

Each ring consists of a number of DMQA nanowires. Neither the distance between adjacent rings nor the density of every nanowire ring is entirely constant, and both of decrease steadily with increasing proximity to the center of the central contact. The average length of as-prepared DMQA nanowires is about 30–40 μm, and their diameter is about 200–300 nm. The gradient concentric ring patterns described here are highly reproducible.

Figure 3 shows that the spacing and the density (defined as the number of nanowires per unit length along the

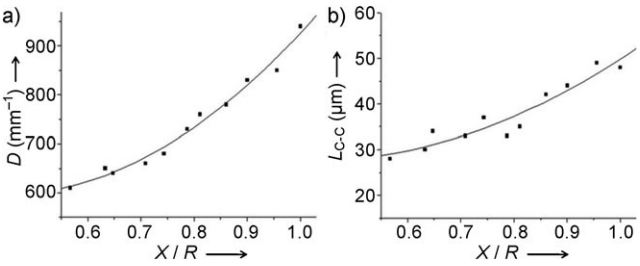

Figure 3. a) *D* and b) $L_{c\text{-}c}$ as a function of *X*/*R* (see text for definitions of symbols).

circumferential direction) of the nanowire array both increase with increasing proximity to the central lens/slide contact. Here *X* is the distance from the center of the lens/slide contact (see Figure 1 b) and *R* is the radius of the outermost ring. The SEM images at three typical positions for the solution with $C = 0.10$ mmol L^{-1} are shown in Figure S1 (Supporting Information). As the solution front moves inward due to evaporative loss of chloroform, both the distance between adjacent arrays of DMQA nanowires $L_{C\text{-}C}$ and the density of the nanowires *D* decrease progressively from $L_{C\text{-}C} = 48$ μm and $D = 940$ mm^{-1} at $X = 5500$ μm to $L_{C\text{-}C} = 35$ μm and $D = 760$ mm^{-1} at $X = 4463$ μm and to $L_{C\text{-}C} = 28$ μm and $D = 610$ mm^{-1} at $X = 3120$ μm (Figure 3). Thus, the rings of DMQA nanowires show gradation in spacing and density. The density and spacing of concentric DMQA rings in the outermost region can also be easily tuned by simply varying the volume of DMQA solution loaded into the lens/slide contact. For example, concentric rings with mean intervals of 50 and 32 μm could be prepared by adding 150 and 100 μL of DMQA solution into the gap between these two objects, respectively.

The concentration of DMQA in chloroform could have potential effects on the formation of ordered concentric rings of organic nanowires. Figure 4 shows two DMQA nanowire patterns (one in Figure 4 a, b and the other in Figure 4 c) at the same outermost region (*X*3) of the substrate which were obtained at different concentrations. Concentric rings of DMQA nanowires could be made at solution concentrations higher than 0.05 mmol L^{-1}. For dilute solutions, a film with ordered organic nanowires was formed, and these nanowires were continuous and oriented parallel to the solution flow. For concentric ring patterns, the spacing and density of the arrays of nanowires could be tuned by changing the initial solution concentration. For example, the intervals could be varied from 150 to 70 μm and the density from (1000 ± 100) to (700 ± 100) mm^{-1} by simply varying the initial solution concentration from 0.20 to 0.10 mmol L^{-1} (Figure 4 a and b). Under the experimental conditions, the saturation concentration of DMQA in chloroform was about (0.23 ± 0.02) mmol L^{-1}. In most instances, a subsaturation concentration was use to give ordered concentric ring patterns of organic nanowires. For DMQA, an optimal concentration around 0.10–0.20 mmol L^{-1} was found. To study the effect of concentration on formation of ring patterns, photoluminescence (PL) properties of DMQA solutions with different concentrations were investigated. As the concentration of

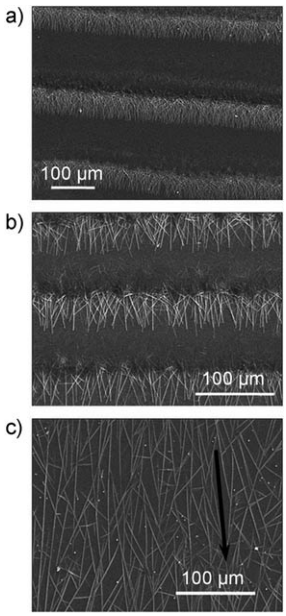

Figure 4. SEM images at position *X*3 of the DMQA nanowire arrays obtained at concentrations of a) 0.2, b) 0.1, and c) 0.05 mM. The black arrow indicates the direction of solution flow (c).

DMQA increased from 0.01 to 0.2 mmol L^{-1}, the emission of DMQA in chloroform underwent a redshift from 539 to 553 nm (Figure S2, Supporting Information). The peak shift could be due to the strong π–π interaction between molecular aggregates. When the concentration was increased to 0.3 mmol L^{-1} or higher, DMQA nanowires formed in solution. The as-obtained nanosuspension exhibited similar PL spectra but with weaker emission than the saturated solution.

The assembly of DMQA nanowires on the substrate to form well-ordered concentric ring patterns may depend on many factors such as evaporation rate, initial solution concentration, nucleation, rate of crystal growth, and solute–substrate interactions. However, periodic temporal–spatial variations of DMQA concentration in the meniscus area should play an important role in pattern formation. The change in concentration leads to periodic precipitation and deposition on the substrate. On the other hand, crystal formation causes two different movement modes, namely, stick–slip motion and fingering instability,[50–53] which both contribute to the ordered micrometer-scale patterns.

The motion of the contact line is governed by the balance between pinning and depinning forces. The pinning force mainly reflects the friction or stiction force preventing shrinkage of the droplet, which is a linear function of the total length of the contact line and the amount of crystal formation.[54] The depinning force is the capillary force caused by surface tension of the solvent, which tends to make the contact line recede. Both of these forces are strongly influenced by DMQA concentration in solution. During the evaporation process, an outward solution flow diffuses from the bulk to replenish the highest evaporation losses at the perimeter, which also takes DMQA molecules from the bulk solution. Therefore, DMQA concentration in the meniscus becomes increasingly higher. When it reaches a certain threshold value of C_p, DMQA molecules begin to form nanocrystals and deposit on the substrate. This roughens the surface, the pinning force surpasses its counterforce, and a stick line begins to form. During this process, DMQA solution in the meniscus is continuously fed from the bulk solution, while DMQA nanocrystals deposit at the contact line, and competition between the two events makes the concentration in the meniscus first increase and then decrease slowly. Therefore, more and more DMQA nanocrystals deposit on the substrate. However, the contact line does not remain pinned for the entire duration. As the solution wets the deposit, the interface slowly changes its convex curvature to concave near the deposit, and hence a dimpled fluid interface occurs near the nanocrystals. Then the depinning force increases quickly and exceeds the pinning force again. As a result, the contact line begins to move, and thus a new ring develops. The solution hence recovers the initial DMQA concentration C_0 (note that the initial concentration C_0 gradually decreases with time, and thus regular patterns can hardly be obtained in the central area). The process repeats over and over until it reaches the central contact area (Figure 5).

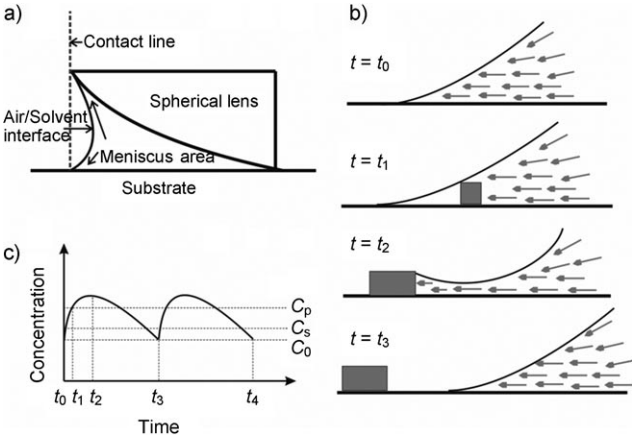

Figure 5. a) Illustration of DMQA in $CHCl_3$ solution in a sphere-on-flat configuration. b) Solution flows in the meniscus area at different times. c) Trend of concentration with time when stick–slip motion occurs.

As the sticking event occurs, migration of DMQA molecules into the thin meniscus area occurs, which may be driven by a fingering convection flow.[41,52] The convection is caused by both temperature and concentration gradients originating from evaporation of the solvent. In our experiments, the difference in temperature between the edge of the solution in the confined geometry and the bulk solution is as high as 2.7 °C. Due to the fingering instability of the dimpled thin film, DMQA molecules quickly agglomerate and self-assemble into 1D organic nanowires in the meniscus area due to strong intermolecular π–π interaction. On the other hand, the alignment of self-assembled DMQA nanowires is always perpendicular to the contact line owing to the convection flow. At a high concentration, more DMQA nanocrystals are deposited at the contact line; therefore, deposition not only

provides a strong pinning force to balance the depinning force to produce a stick–slip motion, but also serves as a nucleation point for DMQA nanowires. At a low concentration such as 0.05 mmol L^{-1} the amount of deposition is so small that no efficient pinning force can be realized to balance its counterforce. Limited deposition can only serve to provide nucleation points for growth of organic nanowires. On the other hand, the depinning force only leads to a fingering convection flow. Hence, a continuous and ordered DMQA nanowire film is obtained (Figure S3b, Supporting Information).[41]

The facile evaporation approach reported here can also be applied to prepare well-aligned organic nanowires directly from a homogenous solution. This greatly reduces material consumption and the cost for fabricating nanoscale devices. Besides, well-organized concentric rings of nanowires also can be formed by the evaporation of several other organic compounds, such as SQ and PTCDI (Figure S4, Supporting Information). In these experiments, two important factors determine formation of nanowires of these compounds in concentric rings: saturation concentration and strong intermolecular interaction. The concentration of the solution is usually between 0.1 and 0.3 mmol L^{-1}. Too high or too low a concentration may lead to an irregular deposition pattern on the substrate. However, organic semiconductor compounds usually have planar aromatic skeletons, and thus delocalized electrons would facilitate 1D self-assembly and formation of organic nanowires. Further investigations will be to generalize the factors affecting the formation of organic nanowires.

The formation of concentric rings of nanowires is also affected by the substrate, which must be at least partially wettable by the evaporated solvent. Therefore, a solvophilic surface is preferred for the formation of these nanowires. For example, in our experiments, the contact angles of CH_2Cl_2 and $CHCl_3$ on the glass substrate are 11 and 14°, respectively. Such a small angle can help to form a well-defined, pinned contact line. In addition, well-ordered concentric rings of nanowires can also be obtained on the surfaces of Si wafer, quartz, and substrates with prefabricated electrode arrays. The inset of Figure 6 shows four nanowires of DMQA deposited across Au electrodes on SiO_2 (300 nm thick)/Si substrate. The *I–V* characteristic of such a parallel device was measured, and the slope of the curve was about 3.1×10^{-12} S. Although the conductivity of DMQA nanowires is not as high as expected, the simple evaporation method makes it possible to grow large-area arrays of organic nanowires directly onto prefabricated electrodes and is applicable to a variety of optoelectronic devices.

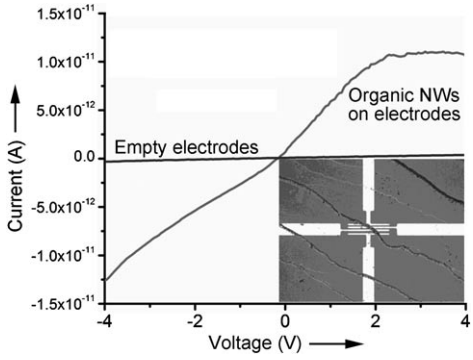

Figure 6. *I–V* curves of DMQA nanowires and the bare electrode. Inset: optical micrograph of DMQA nanowires deposited across electrodes.

In conclusion, we have developed a novel approach to prepare regular concentric rings of ordered and aligned organic nanowires by simply allowing solvent to evaporate in a confined geometry. The confined geometry provides a unique environment for controlling the flow within the evaporating droplet, which, in turn, regulates the pattern formation of nanowires. The density, length, and periodicity of the namowire arrays can be tuned by controlling the evaporation rate. The present one-step approach can serve as a general approach for the growth and patterning of organic nanostructures, and is potentially a low-cost and easily scalable approach for large-scale fabrication of organic devices with 2D nanowires. The self-organized patterns of molecular organic semiconductor over a large area have potential applications in variety of optoelectronic devices, such as OFETs and biosensors.

Experimental Section

N,*N*′-Dimethylquinacridone (DMQA) was synthesized from quinacridone and iodomethane.[15] The crude product was purified by sublimation and then characterized by IR and NMR spectroscopy and EIMS. 2,4-Bis[4-(*N*,*N*-dimethylamino)phenyl] squaraine (SQ) and perylene tetracarboxylic diimide (PTCDI) were also synthesized in-house and characterized by IR and NMR spectroscopy and EIMS. Dichloromethane and chloroform were distilled from CaH_2 just prior to use. All silicon and glass substrates were cleaned several times by sonication in acetone for one hour and dried in an oven. The cleaned substrates were then treated with oxygen plasma right before use.

The solvent evaporation process and optical micrographs were observed with a polarized microscope (Olympus BX51) with attached digital camera (Olympus C-5060). The morphologies of the nanostructures were observed with a field-emission scanning electron microscope (FESEM, Hitachi S-4300), operated at an accelerating voltage of 5 kV. To minimize sample charging, a thin layer of Au was deposited onto the samples before SEM examination. FL spectra were measured on a Hitachi F-4500 spectrophotometer.

Received: November 12, 2010
Published online: February 23, 2011

Keywords: confined-space effects · evaporation · nanostructures · self-assembly · semiconductors

[1] C. W. Tang, S. A. Vanslyke, *Appl. Phys. Lett.* **1987**, *51*, 913.
[2] Y. S. Zhao, C. Di, W. Yang, G. Yu, Y. Liu, J. Yao, *Adv. Funct. Mater.* **2006**, *16*, 1985.
[3] A. Tsumura, H. Koezuka, T. Ando, *Appl. Phys. Lett.* **1986**, *49*, 1210.
[4] C. Reese, Z. Bao, *Mater. Today* **2007**, *10*, 20.
[5] S. Liu, W. M. Wang, A. L. Briseno, S. C. B. Mannsfeld, Z. Bao, *Adv. Mater.* **2009**, *21*, 1217.
[6] S. Liu, H. A. Becerril, M. C. LeMieux, W. M. Wang, J. H. Oh, Z. Bao, *Adv. Mater.* **2009**, *21*, 1266.
[7] L. Schmidt-Mende, A. Fechtenkötter, K. Müllen, E. Moons, R. H. Friend, J. D. MacKenzie, *Science* **2001**, *293*, 1119.
[8] F. Yang, K. Sun, S. R. Forrest, *Adv. Mater.* **2007**, *19*, 4166.

[9] F. Yang, S. R. Forrest, *ACS Nano* **2008**, *2*, 1022.
[10] T. Naddo, Y. Che, W. Zhang, K. Balakrishnan, X. Yang, M. Yen, J. Zhao, J. S. Moore, L. Zang, *J. Am. Chem. Soc.* **2007**, *129*, 6978.
[11] Y. Che, X. Yang, S. Loser, L. Zang, *Nano Lett.* **2008**, *8*, 2219.
[12] T. Q. Nguyen, R. Martel, P. Avouris, M. L. Bushey, L. Brus, C. Nuckolls, *J. Am. Chem. Soc.* **2004**, *126*, 5234.
[13] G. D. Pantoş, P. Pengo, J. K. M. Sanders, *Angew. Chem.* **2007**, *119*, 198; *Angew. Chem. Int. Ed.* **2007**, *46*, 194.
[14] H. B. Liu, Y. L. Li, S. Q. Xiao, H. Y. Gan, T. G. Jiu, H. M. Li, L. Jiang, D. B. Zhu, D. P. Yu, B. Xiang, Y. F. Chen, *J. Am. Chem. Soc.* **2003**, *125*, 10794.
[15] X. J. Zhang, X. H. Zhang, B. Wang, C. Y. Zhang, J. C. Chang, C. S. Lee, S. T. Lee, *J. Phys. Chem. C* **2008**, *112*, 16264.
[16] X. J. Zhang, X. H. Zhang, K. Zou, C. S. Lee, S. T. Lee, *J. Am. Chem. Soc.* **2007**, *129*, 3527.
[17] K. Takazawa, Y. Kitahama, Y. Kimura, G. Kido, *Nano Lett.* **2005**, *5*, 1293.
[18] Y. Yamamoto, T. Fukushima, Y. Suna, N. Ishii, A. Saeki, S. Seki, S. Tagawa, M. Taniguchi, T. Kawai, T. Aida, *Science* **2006**, *314*, 1761.
[19] Y. S. Zhao, J. Xu, A. Peng, H. Fu, Y. Ma, L. Jiang, J. Yao, *Angew. Chem.* **2008**, *120*, 7411; *Angew. Chem. Int. Ed.* **2008**, *47*, 7301.
[20] Y. S. Zhao, A. Peng, H. Fu, Y. Ma, L. Jiang, *Adv. Mater.* **2008**, *20*, 1661.
[21] X. J. Zhang, J. S. Jie, W. F. Zhang, C. Y. Zhang, L. B. Luo, Z. B. He, X. H. Zhang, W. J. Zhang, C. S. Lee, S. T. Lee, *Adv. Mater.* **2008**, *20*, 2427.
[22] S. C. B. Mannsfeld, A. Sharei, S. Liu, M. E. Roberts, Z. Bao, *Adv. Mater.* **2008**, *20*, 4044.
[23] P. Yang, *Nature* **2003**, *425*, 243.
[24] D. Whang, S. Jin, Y. Wu, C. M. Lieber, *Nano Lett.* **2003**, *3*, 1255.
[25] A. Tao, F. Kim, C. Hess, J. Goldberger, R. R. He, Y. G. Sun, Y. N. Xia, P. D. Yang, *Nano Lett.* **2003**, *3*, 1229.
[26] A. R. Tao, J. X. Huang, P. D. Yang, *Acc. Chem. Res.* **2008**, *41*, 1662.
[27] L. Sardone, V. Palermo, E. Devaux, D. Credgington, M. de Loos, G. Marletta, F. Cacialli, J. Van Esch, P. Samori, *Adv. Mater.* **2006**, *18*, 1276.
[28] M. Li, R. B. Bhiladvala, T. J. Morrow, J. A. Sioss, K. K. Lew, J. M. Redwing, C. D. Keating, T. S. Mayer, *Nat. Nanotechnol.* **2008**, *3*, 88.
[29] G. Z. Piao, F. Kimura, T. Kimura, *Langmuir* **2006**, *22*, 4853.
[30] P. A. Smith, C. D. Nordquist, T. N. Jackson, T. S. Mayer, B. R. Martin, J. Mbindyo, T. E. Mallouk, *Appl. Phys. Lett.* **2000**, *77*, 1399.
[31] X. F. Duan, Y. Huang, Y. Cui, J. F. Wang, C. M. Lieber, *Nature* **2001**, *409*, 66.
[32] O. Giraldo, J. P. Durand, H. Ramanan, K. Laubernds, S. L. Suib, M. Tsapatsis, S. L. Brock, M. Marquez, *Angew. Chem.* **2003**, *115*, 3011; *Angew. Chem. Int. Ed.* **2003**, *42*, 2905.
[33] C. Y. Zhang, X. J. Zhang, X. H. Zhang, X. Fan, J. S. Jie, J. C. Chang, C. S. Lee, W. J. Zhang, S. T. Lee, *Adv. Mater.* **2008**, *20*, 1716.
[34] N. L. Liu, Y. Zhou, L. Wang, J. B. Peng, J. Wang, J. Pei, Y. Cao, *Langmuir* **2009**, *25*, 665.
[35] A. M. Kalsin, M. Fialkowski, M. Paszewski, S. K. Smoukov, K. J. M. Bishop, B. A. Grzybowski, *Science* **2006**, *312*, 420.
[36] C. J. Brinker, Y. F. Lu, A. Sellinger, H. Y. Fan, *Adv. Mater.* **1999**, *11*, 579.
[37] R. D. Deegan, O. Bakajin, T. F. Dupont, G. Huber, S. R. Nagel, T. A. Witten, *Nature* **1997**, *389*, 827.
[38] R. D. Deegan, *Phys. Rev. E* **2000**, *61*, 475.
[39] R. D. Deegan, O. Bakajin, T. F. Dupont, G. Huber, S. R. Nagel, T. A. Witten, *Phys. Rev. E* **2000**, *62*, 756.
[40] S. W. Hong, J. Xu, and Z. Lin, *Nano Lett.* **2006**, *6*, 2949.
[41] J. Xu, J. Xia, Z. Lin, *Angew. Chem.* **2007**, *119*, 1892; *Angew. Chem. Int. Ed.* **2007**, *46*, 1860.
[42] S. W. Hong, M. Byun, Z. Lin, *Angew. Chem.* **2009**, *121*, 520; *Angew. Chem. Int. Ed.* **2009**, *48*, 512.
[43] D. M. Kuncicky, R. R. Naik, O. D. Velev, *Small* **2006**, *2*, 1462.
[44] C. S. Ozkan, Z. L. Wang, *Small* **2006**, *2*, 1322.
[45] C. Y. Zhang, X. J. Zhang, X. H. Zhang, X. M. Ou, W. F. Zhang, J. S. Jie, J. C. Chang, C. S. Lee, S. T. Lee, *Adv. Mater.* **2009**, *21*, 4172.
[46] T. Shichiri, M. Suezaki, T. Inoue, *Chem. Lett.* **1992**, 1717.
[47] J. Shi, C. W. Tang, *Appl. Phys. Lett.* **1997**, *70*, 1665.
[48] E. M. Gross, J. D. Anderson, A. F. Slaterbeck, S. Thayumanavan, S. Barlow, Y. Zhang, S. R. Marder, H. K. Hall, M. Flore Nabor, J. F. Wang, E. A. Mash, N. R. Armstrong, R. M. Wightman, *J. Am. Chem. Soc.* **2000**, *122*, 4972.
[49] J. Zambounis, J. Mizuguchi, PCT International Application WO 9608536A1, **1996**.
[50] A. M. Cazabat, F. Heslot, S. M. Troian, P. Carles, *Nature* **1990**, *346*, 824.
[51] I. Leizerson, S. G. Lipson, A. V. Lyushnin, *Langmuir* **2004**, *20*, 291.
[52] J. X. Huang, F. Kim, A. R. Tao, S. Connor, P. D. Yang, *Nat. Mater.* **2005**, *4*, 896.
[53] O. Karthaus, L. Grasjo, N. Maruyama, M. Shimomura, *Chaos* **1999**, *9*, 308.
[54] P. G. de Gennes, *Rev. Mod. Phys.* **1985**, *57*, 827.

